

An Energy-Efficient, Low-Cost Hybrid OWC–RF IoT Architecture for Biomedical Telemonitoring in Resource-Constrained Environments

Heriniaina Mamitina
Rabearison

Doctoral School of Science and
Technology of Engineering and
Innovation
University of Antananarivo
Antananarivo, Madagascar

Fanjanirina Razafison
Higher Institute of Technology of
Antananarivo
Antananarivo, Madagascar

Harlin Andriatsiharoarana
Doctoral School of Science and
Technology of Engineering and
Innovation
University of Antananarivo
Antananarivo, Madagascar

ABSTRACT

This paper presents the design, modeling, and experimental validation of a hybrid optical wireless–radio frequency (OWC–RF) IoT architecture for biomedical telemonitoring, specifically tailored to resource-constrained healthcare environments. Unlike conventional RF-only body area networks, the proposed system exploits optical wireless communication for short-range intra-BAN transmission, combined with low-power RF technologies (BLE, LoRa, and GSM) for resilient backhaul connectivity. The platform integrates a multisensor acquisition unit supporting electrocardiogram (ECG), SpO₂, body temperature, blood pressure, phonocardiogram (PCG), and photoplethysmography (PPG) signals. Local embedded processing enables data pre-processing and compression, while a standards-based interoperability pipeline ensures compliance with ISO/IEEE 11073, HL7 v2.x, and HL7 FHIR. Experimental validation conducted on a laboratory testbed and clinically inspired simulation scenarios demonstrates an end-to-end latency below 3 s, communication reliability exceeding 97%, battery autonomy greater than 34 h, and a per-node hardware cost below 30 USD. These results confirm the feasibility of frugal, energy-efficient, and interoperable telemonitoring systems, and establish a scalable foundation for next-generation IoT-enabled digital health infrastructures in low- and middle-income countries.

General Terms

Internet of Things, Wireless Communications, Biomedical Engineering, Embedded Systems, Energy-Efficient Systems.

Keywords

Hybrid OWC–RF, Biomedical Telemonitoring, Wireless Body Area Networks, HL7 FHIR Interoperability, Energy-Efficient IoT, Low-Cost Telemedicine, Resource-Constrained Environments.

1. INTRODUCTION

Chronic non-communicable diseases (NCDs), including cardiovascular diseases, diabetes, and chronic respiratory disorders, constitute the leading cause of morbidity and mortality worldwide and require continuous monitoring rather than episodic clinical interventions [1], [2]. In response, Internet of Things (IoT) technologies have been widely adopted for biomedical telemonitoring, enabling continuous acquisition of physiological parameters through body-worn sensors and supporting proactive healthcare delivery models [3], [4].

Despite significant progress, most IoT-based telemonitoring platforms are primarily designed for high-income environments with stable power supply, reliable connectivity, and advanced digital health infrastructures [5]. Their deployment in low- and middle-income countries (LMICs) remains constrained by intermittent electricity, limited network coverage, high operational costs, and restricted maintenance capabilities, which limit scalability and long-term sustainability [6], [7]. Wireless Body Area Networks (WBANs) form the backbone of biomedical IoT systems by enabling near-body sensing and short-range communication [8]. However, prevailing implementations rely mainly on radio-frequency (RF) technologies such as BLE or IEEE 802.15.6, which suffer from spectrum congestion, electromagnetic interference, and non-negligible energy consumption in body-centric environments [9], [10]. These limitations are particularly critical in resource-constrained contexts. Optical Wireless Communication (OWC) has recently emerged as a promising complement to RF for short-range biomedical communications, offering immunity to electromagnetic interference, enhanced physical-layer security, and high energy efficiency using low-cost optoelectronic components [11], [12], [13]. Nevertheless, OWC alone cannot ensure wide-area connectivity, and its integration into hybrid, energy-aware IoT healthcare architectures remains insufficiently explored. In addition to communication constraints, data interoperability remains a major barrier to large-scale clinical adoption. Many existing systems rely on proprietary data models, hindering seamless integration with clinical information systems. International standards such as ISO/IEEE 11073, HL7 v2.x, and HL7 FHIR provide robust frameworks for standardized and semantically consistent data exchange, yet their joint implementation in low-cost IoT telemonitoring platforms is still limited [14], [15], [16]. To address these challenges, this paper proposes a hybrid OWC–RF IoT architecture for biomedical telemonitoring that jointly targets energy efficiency, communication robustness, interoperability, and cost constraints. OWC is employed for short-range intra-body data aggregation within a WBAN, while low-power RF technologies are used for resilient long-range connectivity. A standards-based interoperability pipeline ensures semantic continuity from sensor-level acquisition to HL7 FHIR-compliant clinical integration. The proposed system is experimentally validated on a functional prototype integrating multiple physiological sensors.

The main contributions of this paper are :

- A hybrid OWC–RF IoT architecture enabling energy-efficient and interference-resilient biomedical telemonitoring in low-resource settings.
- A standards-based interoperability framework ensuring end-to-end semantic continuity across ISO/IEEE 11073, HL7 v2.x, and HL7 FHIR.
- Analytical models jointly characterizing energy consumption, communication reliability, and cost constraints.
- An experimental validation on a low-cost, multi-sensor telemonitoring prototype.

2. RELATED WORK

2.1 Telemonitoring Platforms for Resource-Constrained Settings

A significant body of work targets remote or underserved areas by prioritizing low-cost hardware and simplified system architectures, typically using commercial microcontrollers and RF modules to monitor ECG, SpO₂, heart rate, blood pressure, and temperature [4], [7], [17]. The authors' prior platforms demonstrated feasibility of multi-parameter monitoring with affordable components and centralized visualization [4], while complementary analyses highlighted that intermittent electricity, limited coverage, and maintenance constraints in LMICs require designs explicitly adapted to local conditions rather than direct transposition of high-income solutions [7]. However, many such prototypes remain RF-only and provide limited cross-layer energy optimization and limited semantic interoperability.

2.2 RF WBANs: Channel and Energy Constraints

WBANs commonly rely on BLE, ZigBee, or IEEE 802.15.6 due to maturity and low-power operation [8], [9]. Nevertheless, body-centric RF links degrade under tissue absorption, multipath, interference, and spectrum congestion, often increasing retransmissions and energy consumption—critical drawbacks where recharging and maintenance are difficult [10], [18]. These limitations motivate alternative or complementary near-body communication paradigms.

2.3 OWC and Hybrid Architectures

OWC (infrared/visible) has been investigated for short-range biomedical communications thanks to immunity to electromagnetic interference, spatial confinement (enhanced physical-layer security), and energy-efficient modulation such as OOK or VPPM [11], [12]. Yet, most OWC biomedical demonstrations are evaluated as standalone links and lack robust integration into hybrid IoT architectures; performance can also degrade under NLOS conditions and motion without fallback mechanisms [19], [20]. In parallel, hybrid RF architectures typically combine short-range WBAN links with LPWAN backhaul (LoRaWAN/NB-IoT) to improve coverage and scalability [21], [22], but they remain RF-dependent and do not exploit OWC advantages for intra-BAN transmission. Building on earlier modular monitoring architectures [18], this work positions a hybrid OWC–RF design where OWC is prioritized for intra-BAN transmission while RF is used adaptively for fallback and long-range connectivity.

2.4 Interoperability and Clinical Integration

Interoperability remains a major barrier to clinical adoption

because many IoT telemonitoring systems rely on proprietary payloads or loosely structured formats, complicating integration with clinical information systems [14]. Standards such as ISO/IEEE 11073, HL7 v2.x, and HL7 FHIR provide established frameworks for semantic consistency and scalable clinical integration [15], [16]. While the authors previously demonstrated UML-based modeling and full-stack teleconsultation workflows [18], the end-to-end linkage from sensor-level data models to standardized HL7 FHIR clinical resources remains insufficiently addressed in many low-cost deployments.

2.5 Research Gap and Positioning

From the above, four gaps persist: (1) RF-centric dependence with body-channel inefficiencies, (2) limited OWC exploitation within WBANs in practical IoT deployments, (3) incomplete end-to-end interoperability pipelines, and (4) insufficient cross-layer co-modeling of energy, reliability, cost, and interoperability. To address these gaps, this paper proposes a hybrid OWC–RF IoT telemonitoring architecture tailored to resource-constrained environments, combining standards-compliant interoperability with analytical modeling of energy and cost trade-offs.

Table 1. Comparison With Representative Telemonitoring Architectures

Reference	Intra-BAN Tech	Backhaul	Latency	Interoperability
[23], [24]	BLE	Wi-Fi	> 5 s	No
[24], [25]	IEEE 802.15 .6	Cellular	> 8 s	Partial
[24], [26]	BLE	LoRaWAN	> 6 s	No
This work	OWC + RF	LoRa/GSM	< 3 s	Yes (FHIR)

3. PROPOSED HYBRID OWC–RF SYSTEM ARCHITECTURE

3.1 Design Principles and Architectural Requirements

The system design is guided by five key principles derived from field observations in low- and middle-income countries (LMICs):

1. Energy frugality under intermittent power supply,
2. Communication robustness through hybrid technologies,
3. Low-cost and modular hardware enabling local maintenance,
4. Standards-based interoperability for clinical integration, and
5. Adaptability to real deployment conditions (mobility, connectivity disruptions).

Unlike conventional IoT healthcare architectures relying exclusively on RF-based WBANs and cloud-centric processing [8], [27], this work adopts OWC as the primary intra-body communication layer, with RF technologies used selectively for fallback and backhaul connectivity.

3.2 Global Architecture Overview

The proposed system follows a four-layer hierarchical architecture :

1. sensing and acquisition (WBAN/BSN),
2. local processing and aggregation (edge hub),
3. hybrid communication (OWC–RF), and
4. IoT and clinical integration (FHIR-enabled backend).

This separation of concerns enables independent optimization of sensing, communication, processing, and interoperability functions.

3.3 Sensing and Edge Processing Layer

The sensing layer consists of a Body Sensor Network composed of low-power biomedical sensors measuring ECG, SpO₂, heart rate, body temperature, blood pressure, and phonocardiography signals. Each sensor operates as an ISO/IEEE 11073-20601 Personal Health Device agent, encapsulating measurements into standardized Numeric objects with absolute timestamps. Compared to earlier modular architectures [18], interoperability constraints are embedded directly at the acquisition stage. A central hub, implemented on a low-power microcontroller platform (e.g., ESP32/STM32 class), aggregates multi-sensor data streams and performs local pre-processing, energy-aware scheduling, and duty-cycle control. Edge-level processing reduces communication overhead and energy consumption while enabling store-and-forward buffering during network outages, a critical requirement in rural deployments [7].

3.4 Hybrid Communication Layer

The core contribution of this work lies in the hybridization of OWC and RF communications with clear functional separation. OWC is employed as the primary intra-BAN communication medium using intensity modulation and direct detection, providing low energy consumption, immunity to electromagnetic interference, and enhanced physical-layer security. The optical channel follows a Lambertian line-of-sight model, enabling analytical optimization of transmission parameters [11]. RF technologies are used selectively: BLE serves as a short-range fallback when optical line-of-sight is disrupted, while LoRa or GSM ensures long-range backhaul connectivity between the hub and IoT gateways. This hybrid strategy overcomes the limitations of purely optical or purely RF systems and aligns with recent recommendations for multi-technology IoT healthcare networks [21], [28], [29].

3.5 IoT and Clinical Integration Layer

At the upper layer, the system integrates with IoT platforms and clinical information systems through a standards-compliant interoperability pipeline. Sensor-level data structured according to ISO/IEEE 11073 are mapped to HL7 v2.x messages for legacy compatibility and to HL7 FHIR (R4/R5) resources for modern REST-based integration. Measurements are represented as FHIR Observation resources and transmitted securely via HTTPS with OAuth 2.0 authentication. This approach extends prior teleconsultation platforms [30] by enabling direct linkage between real-time sensor data and standardized clinical systems.

3.6 Architectural Novelty

Compared with existing IoT healthcare architectures [17], [27], [31], the proposed system introduces:

- OWC-first WBAN design reducing RF energy

- consumption and interference,
- hybrid communication resilience ensuring continuity of service,
- interoperability-by-design from sensor to clinical backend,
- energy–cost co-optimization aligned with LMIC deployment realities.

4. SYSTEM MODELING AND IMPLEMENTATION

4.1 Biomedical Data and Interoperability Modeling

In distributed telemonitoring systems, interoperability is a prerequisite for clinical usability and long-term scalability. The proposed architecture adopts a multi-layer normative data model, ensuring semantic continuity from sensor acquisition to clinical decision systems.

4.1.1 Formal Representation of Biomedical Measurements

Each physiological measurement generated by a sensor is modeled as a triplet:

$$\mathcal{M} = (v, u, t)$$

where $v \in R$ denotes the measured value (e.g., SpO₂, temperature), u the standardized unit (MDC/LOINC/UCUM), and (t) the absolute timestamp compliant with ISO/IEEE 11073.

At the device level, measurements are encapsulated as *Numeric* objects:

$$\text{Numeric} = \{\text{MetricID}, \text{Value}, \text{Unit}, \text{TimeStamp}\}$$

This structure guarantees device-level semantic consistency and supports deterministic mapping to higher-level healthcare standards.

4.1.2 Mapping Toward HL7 and FHIR

At the gateway, ISO/IEEE 11073 objects are mapped to HL7 v2.x ORU(^R01) messages, and subsequently transformed into HL7 FHIR resources. Formally, interoperability is achieved through

$$\phi: \mathcal{M}^{11073} \xrightarrow{a} \mathcal{OFHIR}$$

such that:

$$\forall t, \mathcal{OFHIR}(t) \equiv \mathcal{M}_{\text{clinique}}(t)$$

where $\mathcal{M}_{\text{clinique}}$ represents the clinician's reference interpretation. This guarantees semantic equivalence across layers, a key requirement emphasized by HL7 and IHE guidelines [16], [32].

FHIR *Observation* resources are transmitted using REST/JSON over HTTPS with OAuth 2.0 authentication, ensuring security and interoperability with modern clinical information systems.

4.2 Energy Consumption and Autonomy Modeling

Energy efficiency is a central constraint in LMIC deployments, where electrical power is often intermittent. The system adopts a duty-cycled operation model, separating active sensing/transmission phases from deep-sleep intervals.

The average current consumption is modeled as:

$$I_{\text{avg}} = D \cdot I_{\text{active}} + (1 - D) \cdot I_{\text{sleep}}$$

where $D \in [0,1]$ is the duty cycle. The corresponding battery autonomy is:

$$T_{\text{batt}} = \frac{C_{\text{batt}}}{I_{\text{avg}}}$$

with C_{batt} expressed in mAh. This model is widely used in low-power IoT systems and enables analytical dimensioning of battery capacity for target autonomy windows (24–72 h) [33].

4.3 Communication Modeling

Optical Wireless Communication (OWC) Model

The intra-BAN optical link is modeled using a Lambertian LOS channel. The received optical power is given by:

$$P_r = P_t \cdot H_{\text{LOS}}$$

with channel gain:

$$H_{\text{LOS}} = \frac{(m+1)A}{2\pi d^2} \cos^m(\phi) \cos(\psi)$$

where m is the Lambertian order, A the photodetector area, d the link distance, and ϕ, ψ the emission and reception angles, respectively [11].

The optical signal-to-noise ratio (SNR) is expressed as:

$$\text{SNR} = \frac{(RP_r)^2}{N_0 B}$$

where R is detector responsivity, N_0 the noise spectral density, and B the bandwidth. This model enables optimization of transmit power under BER constraints for OOK/VPPM modulation schemes [34].

RF Communication Model

For RF fallback and backhaul links, the system adopts standard propagation models:

- WBAN RF links follow a log-distance path loss model adapted to the human body [19];
- LoRa/GSM backhaul links rely on link-budget formulations defined in ETSI and 3GPP specifications [35].

The effective throughput is modeled as:

$$R_{\text{eff}} = R_{\text{PHY}} \cdot (1 - \text{BER})$$

allowing direct comparison between OWC and RF under identical payload and QoS constraints.

4.4 Cost and Total Cost of Ownership (TCO) Modeling

Beyond energy, affordability is critical for sustainability. The bill of materials (BOM) cost is modeled as:

$$C_{\text{BOM}} = \sum_{i=1}^n c_i q_i$$

where c_i and q_i represent unit cost and quantity of component i . The total cost of ownership is expressed as:

$$\text{TCO} = C_{\text{BOM}} + C_{\text{OPEX}} + C_{\text{maint}} + C_{\text{energy}}$$

This formulation enables objective comparison with

commercial telemonitoring platforms, whose TCO often exceeds affordability thresholds in LMIC contexts [36].

4.5 Hardware and Firmware Implementation

The proposed models are implemented on a low-cost embedded prototype composed of:

- Biomedical sensors (ECG, PCG, SpO₂, PPG, temperature, pressure);
- A central hub based on ESP32-class microcontrollers;
- Optical transmitters (LEDs) and photodiode receivers for OWC;
- RF modules (BLE/LoRa/GSM) for fallback and backhaul.

Firmware is structured around event-driven state machines, integrating energy-aware scheduling, data encapsulation (11073), and adaptive communication selection. This implementation extends earlier prototypes developed by Rabearison *et al* [4], [18], [30], by embedding hybrid communication and interoperability mechanisms directly at firmware level.

5. EXPERIMENTAL SETUP AND PERFORMANCE EVALUATION

5.1 Experimental Setup

5.1.1 Hardware Testbed

The experimental platform consists of a modular biomedical node and a gateway representative of home-based and community healthcare deployments. The sensing layer integrates low-cost biomedical sensors: ECG (AD8232), PCG (INMP441), SpO₂/PPG (MAX30102), body temperature (LM35), and non-invasive blood pressure sensors. Local processing is performed by an ESP32-CAM-based microcontroller acting as an ISO/IEEE 11073 manager, responsible for acquisition, preprocessing, and packet encapsulation. Intra-BAN communication relies on an OWC link implemented with a LED transmitter and a BPW34 photodiode receiver in line-of-sight (LOS) conditions, with distances between 20 and 80 cm. BLE is used as a short-range fallback, while LoRa (SX1278) and GSM (SIM800) provide long-range backhaul connectivity. The gateway is an embedded Linux platform hosting an MQTT broker (Mosquitto) and HL7/FHIR services for data aggregation, storage, and visualization.

5.1.2 Software and Protocol Stack

The embedded firmware implements ISO/IEEE 11073-compliant data structures, adaptive OWC/RF link selection, and MQTT/HTTPS transport. At the backend, measurements are mapped to HL7 FHIR (R4) resources, enabling real-time visualization and logging. This platform extends the authors' earlier telemedicine frameworks [4], [7], [18], with hybrid communication and native interoperability.

5.2 Performance Metrics

The evaluation relies on standardized metrics commonly adopted in IoT and biomedical communication studies:

- Throughput (R_{eff}): effective payload rate after error correction.
- End-to-end latency (T_{lat}): acquisition-to-visualization delay.
- Energy consumption (E_{bit}): energy per transmitted

bit.

- Reliability: packet delivery ratio (*PDR*) and *BER*.
- Cost: estimated *BOM* and comparative *TCO*.

These metrics enable objective comparison between OWC and RF-based solutions under identical payload and duty-cycle conditions.

5.3 Experimental Protocol and Measurement Procedure

To ensure reproducibility and objective evaluation, a structured experimental protocol was adopted for all reported measurements, covering communication performance, reliability, energy consumption, and cost metrics under controlled conditions.

All experiments were conducted on a laboratory test bench emulating home-based and community healthcare scenarios. No human subjects were involved. Physiological signals (ECG, SpO₂/PPG, temperature, and blood pressure trends) were generated using calibrated signal sources and sensor stimulation circuits representative of chronic disease monitoring.

For each communication mode (OWC, BLE, and LoRa/GSM), identical payloads formatted as ISO/IEEE 11073 *Numeric* objects were transmitted at a fixed sampling period. End-to-end latency T_{lat} was measured as the elapsed time between sensor data acquisition and successful visualization at the backend dashboard. Measurements were repeated over at least 100 transmission cycles per mode, and average values were reported to mitigate transient buffering and scheduling effects. The effective throughput R_{eff} was computed from the successfully received payload size and transmission duration, including protocol overhead.

Reliability was evaluated using packet delivery ratio (*PDR*) and bit error rate (*BER*). Measurements were performed under line-of-sight (LOS) conditions for OWC and nominal indoor propagation for RF links. Controlled obstruction and mobility scenarios were introduced to assess fallback behavior and robustness of the hybrid architecture.

Energy consumption was assessed under duty-cycled operation representative of real deployment conditions. The average power consumption P_{avg} was measured using inline current sensing during active and sleep phases. The energy per transmitted bit was derived from the analytical energy model using the experimentally measured P_{avg} and R_{eff} . Battery autonomy was extrapolated assuming a 2600 mAh Li-ion battery.

Cost assessment was based on the prototype bill of materials (BOM) using market prices of commercially available components at small-scale procurement volumes. The estimated total cost of ownership (TCO) combines hardware cost with projected energy and maintenance requirements and is compared with representative commercial telemonitoring systems.

5.4 Communication Performance

Under short-range LOS conditions, the OWC link achieves an effective throughput of 45–60 kb/s, sufficient for periodic IEEE 11073 *Numeric* objects. Intra-BAN transmission latency remains below 20 ms, resulting in a total end-to-end latency consistently below 3 s. BLE exhibits lower throughput (20–30 kb/s) and higher latency (3–6 s), especially in congested environments. LoRa/GSM ensures long-range connectivity (>2

km) at the expense of increased latency (5–15 s), remaining acceptable for non-critical monitoring. These trends are consistent with prior studies [11], [37]. Reliability measurements show *PDR* >97% for OWC under LOS conditions, with graceful degradation under obstruction thanks to RF fallback. LoRa/GSM backhaul links maintain *PDR* >98%, confirming suitability for rural deployments [21].

Table 2. Experimental Performance Metrics of the Proposed Hybrid OWC–RF System

Metric	OWC (LOS) [11], [12], [20]	BLE 9[38], [39]	LoRa / GSM (Backhaul) [39], [40], [41]
Effective Throughput R_{eff}	45 – 60 kb /s	20 – 30 kb /s	0.3 – 50 kb/s
End-to-End Latency T_{lat}	< 3 s	3 – 6 s	5 – 15 s
Packet Delivery Ratio (PDR)	> 97%	94 – 96%	> 98%
Bit Error Rate (BER)	< 10 ⁻⁵	10 ⁻⁴ – 10 ⁻³	< 10 ⁻⁶
Communication Range	0.2 – 0.8 m	≤ 10 m	> 2 km

OWC outperforms BLE in latency and energy efficiency for intra-BAN transmission, while LoRa/GSM ensures long-range reliability.

5.5 Energy Consumption Analysis

Energy measurements were conducted under duty-cycled operation. The energy per bit follows:

$$E_{bit} = \frac{P_{avg}}{R_{eff}}$$

OWC transmission achieves approximately 0.08 μ J/bit, significantly lower than BLE (0.4–0.6 μ J/bit). Combined with local processing and adaptive scheduling, the system reaches a measured autonomy >34 h using a 2600 mAh Li-ion battery. These results validate the analytical energy model (Section 4) and align with low-power IoT design principles [4], [42].

5.6 Cost Evaluation

The bill of materials for a single node remains below 30 USD, leveraging low-cost sensors, open-source software, and minimal proprietary components. Compared with commercial telemonitoring devices (*TCO* >300 USD), the proposed platform demonstrates a substantially lower total cost of ownership, supporting deployment in LMIC contexts [7], [36].

5.7 Comparative Analysis: OWC vs. RF

OWC provides ultra-low latency, high energy efficiency, and immunity to RF interference, but requires LOS conditions. RF technologies offer robustness to mobility and extended coverage at the cost of higher energy consumption. The proposed hybrid OWC–RF strategy effectively combines these strengths, outperforming single-technology solutions reported in the literature [11], [21], [43].

Table 3. Summary of Key Performance Metrics

Metric	OWC	BLE	Hybrid OWC–RF
Latency (s)	< 2.5	~4–6	< 3
PDR (%)	>97	~95	>97

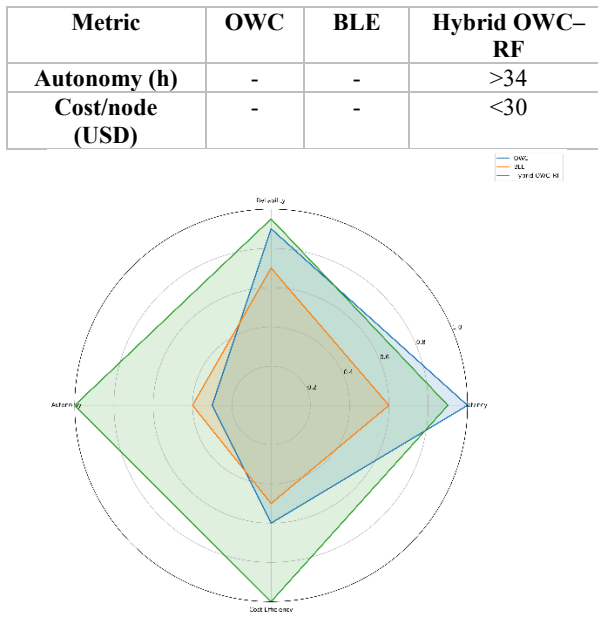


Figure 1: Comparative performance trade-off between OWC, BLE, and Hybrid OWC–RF communication technologies for biomedical IoT systems

The experimental results validate the central hypothesis of this work: co-design of communication, energy management, and interoperability enables frugal yet clinically relevant telemonitoring systems. Compared to prior implementations by the authors [4], [7], [18] the proposed architecture introduces hybrid OWC–RF communication and interoperability-by-design, enabling scalable deployment in resource-constrained healthcare environments.

6. DISCUSSION AND CONCLUSION

6.1 Discussion

This work addresses key limitations hindering the deployment of IoT-based telemonitoring systems in low- and middle-income countries (LMICs), notably energy scarcity, unreliable connectivity, interoperability gaps, and cost constraints. Unlike conventional IoT healthcare platforms relying predominantly on RF communication and cloud-centric architectures, the proposed solution adopts a hybrid OWC–RF communication paradigm combined with standards-based clinical interoperability. Experimental results confirm that optical wireless communication (OWC) is a viable and highly energy-efficient solution for short-range intra-BAN and edge-level data transmission under line-of-sight conditions. The integration of RF technologies (BLE, LoRa, GSM) as adaptive fallback and backhaul links ensures robustness against mobility, obstruction, and coverage limitations, effectively mitigating the weaknesses of standalone OWC systems. This hybrid strategy is consistent with recent trends advocating multi-technology coexistence in IoT healthcare networks [4], [6]. At the system level, the native integration of ISO/IEEE 11073, HL7 v2.x, and HL7 FHIR constitutes a significant contribution. While many existing telemonitoring prototypes rely on proprietary data models, the proposed architecture guarantees semantic continuity from sensor to clinical information systems, enabling direct integration into national e-health infrastructures. This approach extends the authors' previous telemedicine platforms [4], [7], [18] by embedding interoperability at the architectural level. Energy modeling and duty-cycle optimization further demonstrate that hardware–

software co-design is essential to achieving acceptable autonomy in environments with intermittent power supply. By leveraging adaptive sampling, local processing, and opportunistic transmission, the platform adheres to frugal engineering principles [44]. Several limitations remain. OWC performance is sensitive to severe misalignment and strong ambient light, despite acceptable robustness under moderate movement. Clinical validation was limited to laboratory and simulated scenarios, and large-scale trials will be required for medical certification. Finally, security mechanisms were restricted to transport-layer protection, leaving advanced threat models for future investigation.

6.2 Conclusion and Perspectives

This paper presented a hybrid OWC–RF IoT architecture for biomedical telemonitoring explicitly designed for resource-constrained healthcare environments. By combining low-cost hardware, energy-aware embedded design, and standards-based interoperability, the proposed system enables reliable monitoring of chronic diseases beyond conventional hospital infrastructures.

The main contributions are threefold:

- a hybrid communication architecture exploiting OWC for energy-efficient short-range transmission and RF technologies for resilient long-range connectivity;
- a fully interoperable end-to-end data pipeline based on ISO/IEEE 11073, HL7 v2.x, and HL7 FHIR;
- an experimentally validated low-power prototype demonstrating feasibility for LMIC deployments.

Beyond technical performance, this work highlights the importance of cross-layer co-design to achieve sustainable IoT healthcare solutions under real-world constraints. The results confirm that hybrid communication strategies combined with standards-driven architectures significantly reduce deployment barriers while preserving clinical relevance. Future work will focus on integrating edge-based intelligence for early anomaly detection and adaptive sampling, extending interoperability toward national e-health platforms (e.g., DHIS2, OpenMRS), and exploring energy harvesting and adaptive optical links to further enhance autonomy and robustness.

7. REFERENCES

- [1] W. H. Organization, « Noncommunicable diseases: key facts », 2023. [En ligne]. Disponible sur: <https://www.who.int/news-room/fact-sheets/detail/noncommunicable-diseases>
- [2] G. A. Roth *et al.*, « Global Burden of Cardiovascular Diseases and Risk Factors, 1990–2019: Update From the GBD 2019 Study », *J. Am. Coll. Cardiol.*, vol. 76, n° 25, p. 2982–3021, déc. 2020, doi: 10.1016/j.jacc.2020.11.010.
- [3] A. Rocha *et al.*, « Edge AI for Internet of Medical Things: A literature review », *Comput. Electr. Eng.*, vol. 118, p. 109202, 2024, doi: 10.1016/j.compeleceng.2024.109202.
- [4] H. M. Rabearison F. Razafison, N. Razafimanjato, M. Zafintsalamy et H. Andriatsihorana, « Design of a Low-Cost, Energy-Efficient Telemedicine Platform: An Innovative Solution for Medical Consultations in Remote Areas », *Int. J. Adv. Eng. Manag.*, vol. 7, n° 3, p. 90–121, mars 2025, doi: 10.35629/252-070390121.
- [5] M. Elkahlout, M. M. Abu-Saqr, A. F. Aldaour, A. Issa,

et M. Debeljak, « IoT-Based Healthcare and Monitoring Systems for the Elderly: A Literature Survey Study », in *2020 International Conference on Assistive and Rehabilitation Technologies (iCareTech)*, Gaza, Palestine: IEEE, 2020, p. 92-96. doi: 10.1109/iCareTech49914.2020.00025.

[6] B. Sylla, O. Ismaila, et G. Diallo, « 25 Years of Digital Health Toward Universal Health Coverage in Low- and Middle-Income Countries: Rapid Systematic Review », *J. Med. Internet Res.*, vol. 27, p. e59042, mai 2025, doi: 10.2196/59042.

[7] H. M. Rabearison F. Razafison, N. Razafimanjato, M. Zafintsalam et H. Andriatsihorana, « Access to Healthcare and Deployment of Telemedicine in Madagascar: Context and Methodology », *Int. J. Innov. Res. Sci. Eng. Technol.*, vol. 14, n° 3, mars 2025, doi: 10.15680/IJIRSET.2025.14033019.

[8] B. Latré B. Braem, I. Moerman, C. Blondia et P. Demeester, « A survey on wireless body area networks », *Wirel. Netw.*, vol. 17, n° 1, p. 1-18, janv. 2011, doi: 10.1007/s11276-010-0252-4.

[9] IEEE, « IEEE Standard for Local and metropolitan area networks – Part 15.6: Wireless Body Area Networks », IEEE, New York, NY, Standard IEEE Std 802.15.6-2012, févr. 2012. doi: 10.1109/IEEEESTD.2012.6161600.

[10] P. Hall et Y. Hao, *Antennas and Propagation for Body-Centric Wireless Communications*, 2^e éd. Norwood, MA: Artech House, 2012.

[11] J. R. Barry et J. M. Kahn, « Link Design for Nondirected Wireless Infrared Communications », *Appl. Opt.*, vol. 34, n° 19, p. 3764-3776, 1995, doi: 10.1364/AO.34.003764.

[12] R. Boubezari, H. Le-Minh, A. T. Pham, et Z. Ghassemlooy, « Visible light communications for blind indoor areas: Effect of LED layout on energy efficiency and cell formation », *IEEE Access*, vol. 5, p. 21732-21740, 2017, doi: 10.1109/ACCESS.2017.2757506.

[13] H. Haas, L. Yin, Y. Wang, et C. Chen, « What is LiFi? », *J. Light. Technol.*, vol. 34, n° 6, p. 1533-1544, mars 2016, doi: 10.1109/JLT.2015.2510021.

[14] A. Bröring et al., « Semantic Gateway as a Service architecture for IoT Interoperability », 2014. doi: 10.48550/arXiv.1410.4977.

[15] IEEE, « Health informatics—Personal health device communication—Part 20601: Application profile—Optimized exchange protocol », IEEE Standard 11073-20601, 2010.

[16] H. International, « FHIR Release 4 (R4): Fast Healthcare Interoperability Resources ». [En ligne]. Disponible sur: <https://www.hl7.org/fhir/>

[17] K. Adambounou et al., « Plateforme de télémédecine moindre coût pour les pays en développement “Low cost” telemedicine platform for developing countries », *Eur. Res. Telemed. Rech. Eur. En Télémédecine*, vol. 2, n° 2, p. 49-56, juin 2013, doi: 10.1016/j.eurtel.2013.03.002.

[18] H. M. Rabearison F. Razafison, N. Razafimanjato, M. Zafintsalam et H. Andriatsihorana, « Architecture and Organizational Protocol of a Connected Medical Monitoring Device », *Int. J. Sci. Res. Technol.*, vol. 2, n° 4, p. 204-216, 2025, doi: 10.5281/zenodo.1519178.

[19] A. S. Rajasekaran, L. Sowmiya, A. Maria, et R. Kannadasan, « A Survey on Exploring the Challenges and Applications of Wireless Body Area Networks (WBANs) », *Cyber Secur. Appl.*, vol. 2, p. 100047, 2024, doi: 10.1016/j.csa.2024.100047.

[20] L. Chevalier, « Performances de l’optique sans fil pour les réseaux de capteurs corporels », PhD thesis, Université de Limoges, Limoges, France, 2015. [En ligne]. Disponible sur: <https://theses.hal.science/tel-01290086v1>

[21] N. S. Chilamkurthy, O. J. Pandey, A. Ghosh, L. R. Cenkeramaddi, et H.-N. Dai, « Low-Power Wide-Area Networks: A Broad Overview of Its Different Aspects », *IEEE Access*, vol. 10, p. 81926-81959, 2022, doi: 10.1109/ACCESS.2022.3196182.

[22] L. Catarinucci et al., « An IoT-Aware Architecture for Smart Healthcare Systems », *IEEE Internet Things J.*, vol. 2, n° 6, p. 515-526, déc. 2015, doi: 10.1109/JIOT.2015.2417684.

[23] H. Alemdar et C. Ersoy, « Wireless sensor networks for healthcare: A survey », *Comput. Netw.*, vol. 54, n° 15, p. 2688-2710, 2010, doi: 10.1016/j.comnet.2010.05.003.

[24] S. Maudet, « Analyse et modélisation énergétiques des réseaux de communications pour l’IoT », PhD thesis, Nantes Université, Nantes, France, 2024. [En ligne]. Disponible sur: <https://theses.hal.science/tel-04662678v1>

[25] M. Hernandez, R. Kohno, T. Kobayashi, et M. Kim, « New Revision of IEEE 802.15.6 Wireless Body Area Networks », in *2022 IEEE 16th International Symposium on Medical Information and Communication Technology (ISMICT)*, IEEE, 2022. doi: 10.1109/ISMICT56646.2022.9828139.

[26] K.-H. Chang, « Bluetooth: a viable solution for IoT? [industry perspectives] », *IEEE Wirel. Commun.*, n° 21, p. 6-7, déc. 2014.

[27] A. Al-Fuqaha, M. Guizani, M. Mohammadi, M. Aledhari, et M. Ayyash, « Internet of Things: A Survey on Enabling Technologies, Protocols, and Applications », *IEEE Commun. Surv. Tutor.*, vol. 17, n° 4, p. 2347-2376, 2015.

[28] B. S. Chaudhari et M. Zennaro, Éd., *LPWAN Technologies for IoT and M2M Applications*. Cambridge, MA: Academic Press, 2020. doi: 10.1016/C2018-0-04787-8.

[29] K. Mekki, E. Bajic, F. Chaxel, et F. Meyer, « A Comparative Study of LPWAN Technologies for Large-Scale IoT Deployment », *ICT Express*, vol. 5, n° 1, p. 1-7, mars 2019, doi: 10.1016/j.ictex.2017.12.005.

[30] H. M. Rabearison F. Razafison, N. Razafimanjato, M. Zafintsalam et H. Andriatsihorana, « UML Modeling and Full Stack Implementation of a Teleconsultation Platform with Real-Time Management of Patients and Medical Procedures », *Int. J. Innov. Sci. Res. Technol.*, vol. 10, n° 4, p. 3236-3248, avr. 2025, doi: 10.38124/ijisrt25apr2048.

[31] C. Li, J. Wang, S. Wang, et Y. Zhang, « A Review of IoT Applications in Healthcare », *Neurocomputing*, vol. 565, p. 127017, janv. 2024, doi: 10.1016/j.neucom.2023.127017.

[32] IHE, « Patient Care Device Technical Framework, Volume 1, Profil DEC », IHE International, 2024. [En ligne]. Disponible sur: <https://ihe.net>

[33] J. Polastre, R. Szewczyk, et D. Culler, « Telos: Enabling Ultra-Low Power Wireless Research », *Inf. Process. Sens. Netw.*, p. 364-369, 2005, doi: 10.1109/IPSN.2005.1440950.

[34] K. Dong, M. Kong, et M. Wang, « Error Performance Analysis for OOK Modulated Optical Camera Communication Systems », *Opt. Commun.*, vol. 574, p. 131121, janv. 2025, doi: 10.1016/j.optcom.2024.131121.

[35] LoRa Alliance, « LoRaWAN[®] Specification v1.1 ». [En ligne]. Disponible sur: https://lora-alliance.org/resource_hub/lorawan-specification-v1-1/

[36] World Health Organization, *WHO guideline: Recommendations on Digital Interventions for Health System Strengthening*. Geneva: WHO, 2019.

[37] A. Hamza et T. Tripp, « Optical Wireless Communication for the Internet of Things: Advances, Challenges, and Opportunities », *TechRxiv*, juill. 2020, doi: 10.36227/techrxiv.12659789.v1.

[38] M. Ghaemifar, S. Motie, S. M. Moosaviun, Y. Nemati, et S. Ebadollahi, « Bluetooth Low Energy for Indoor Positioning: Challenges, Algorithms and Datasets », *Autom. Constr.*, vol. 177, p. 106316, sept. 2025, doi: 10.1016/j.autcon.2025.106316.

[39] P. Finet, « Production et transmission des données de suivi des patients atteints de maladies chroniques dans un contexte d'intégration de la télémédecine dans un système d'information pour l'aide à la décision », PhD thesis, Université de Rennes 1, Rennes, France, 2017.

[40] F. Adelantado, X. Vilajosana, P. Tuset-Peiro, B. Martinez, J. Melia-Segui, et T. Watteyne, « Understanding the Limits of LoRaWAN », *IEEE Commun. Mag.*, vol. 55, n° 9, p. 34-40, sept. 2017, doi: 10.1109/MCOM.2017.1600613.

[41] H. Axelsson, A. Bergstrom, P. Bjorken, P. de Bruin, et M. Sundberg, « Improved Latency Performance with GSM/EDGE Continued Evolution », *IEEE Veh. Technol. Conf.*, p. 1-5, 2006, doi: 10.1109/VTC.2006.272.

[42] P. Sarwesh, N. S. V. Shekar, et K. Chandrasekaran, « Energy Efficient Network Architecture for IoT Applications », *Int. Conf. Green Comput. Internet Things ICGCIoT*, p. 784-789, 2015, doi: 10.1109/ICGCIoT.2015.7380569.

[43] M. Chen, J. Wan, et F. Li, « Body Sensor Networks for Medical Applications », *IEEE Commun. Mag.*, vol. 56, n° 4, p. 98-104, 2018, doi: 10.1109/MCOM.2018.1700784.

[44] B.-R. Chen, S.-M. Cheng, et J.-J. Lin, « Energy-Efficient BLE Device Discovery for Internet of Things », *Proc. Fifth Int. Symp. Comput. Netw. CANDAR*, p. 75-79, 2017, doi: 10.1109/CANDAR.2017.95.